JOURNAL OF SCIENCE
SAKARYA UNIVERSITY

Sakarya University Journal of Science

ISSN 1301-4048 | e-ISSN 2147-835X | Period Bimonthly | Founded: 1997 | Publisher Sakarya University | http://www.saujs.sakarya.edu.tr/en/

Title: Structural, Microstructural and Electrochemical Characterization of Ni-YSZ Anodes Fabricated from Pechini-Derived Composite Powders

Authors: Buse BİLBEY, Gamze EROL, Aligül BÜYÜKAKSOY
Recieved: 2019-12-13 17:03:19

Accepted: 2020-05-31 14:41:04

Article Type: Research Article
Volume: 24
Issue: 4
Month: August
Year: 2020
Pages: 740-750

How to cite
Buse BİLBEY, Gamze EROL, Aligül BÜYÜKAKSOY; (2020), Structural, Microstructural and Electrochemical Characterization of Ni-YSZ Anodes Fabricated from Pechini-Derived Composite Powders. Sakarya University Journal of Science, 24(4), 740-750, DOI: https://doi.org/10.16984/saufenbilder.659147
Access link
http://www.saujs.sakarya.edu.tr/en/pub/issue/55932/659147

Sakarya University Journal of Science 24(4), 740-750, 2020

Structural, Microstructural and Electrochemical Characterization of Ni-YSZ Anodes Fabricated from Pechini-Derived Composite Powders

Buse BİLBEY[1], Gamze EROL[2], Aligül BÜYÜKAKSOY[*3]

Abstract

The most widely used solid oxide fuel cell (SOFC) anodes, nickel-yttria stabilized zirconia (NiO-YSZ) composites, are generally fabricated by co-sintering of NiO and YSZ powders. In this study, to achieve a longer triple phase boundary length, these composites were fabricated from powders synthesized via an ethylene glycol-based Pechini method. Polymeric precursors of NiO and YSZ were prepared separately and then mixed, dried and calcined 600, 700 and 800°C for 4 hours, in air. NiO and YSZ crystals with average sizes of 26 and 7 nm, respectively were achieved upon calcination at 600 °C. With increasing heat treatment temperature, both the crystal and agglomerate sizes increased, which, in turn, an increased the anode polarization resistances. Electrochemical activities comparable to or higher than anode prepared by co-sintering of powder mixtures were achieved in the anodes prepared by sintering of the composite powders.

Keywords: Solid oxide fuel cells, polymeric precursor, NiO-YSZ, Pechini method

1. INTRODUCTION

Nickel-yttria stabilized zirconia (Ni-YSZ) composites are the most widely used anode materials in solid oxide fuel cells (SOFCs). The interest in Ni-YSZ anodes originates from the excellent electrocatalytic activity of Ni for hydrogen (or hydrocarbon) oxidation, its high electronic conductivity and the high ionic conductivity, as well as the chemical stability of YSZ [1,2,3].

[1]Gebze Technical University, Department of Materials Science and Engineering, 41400 Gebze, Kocaeli. ORCID: https://orcid.org/ 0000-0002-7404-866X. E-mail: bbilbey@gtu.edu.tr
[2]Gebze Technical University, Department of Materials Science and Engineering, 41400 Gebze, Kocaeli. ORCID: https://orcid.org/ 0000-0002-8619-3418. E-mail: gg.gamze.erol@gmail.com
[*]Corresponding Author: aligul@gtu.edu.tr
[3]Gebze Technical University, Department of Materials Science and Engineering, 41400 Gebze, Kocaeli
Gebze Technical University, Institute of Nanotechnology, Gebze, Kocaeli.
ORCID: https://orcid.org/0000-0003-2227-8938

The conventional method to fabricate Ni-YSZ anodes is based on the deposition of an ink consisting of NiO and YSZ powders, as well as solvents and binders onto a previously sintered, dense YSZ electrolyte substrate, followed by sintering at 1100-1300 °C and in-situ reduction into Ni-YSZ [4], as depicted schematically in Figure 1a. Since fuel oxidation takes place at the Ni-YSZ-gas interface, i.e., triple phase boundaries (TPBs), studies have focused on the development of fabrication techniques that would maximize the lengths of these electrocatalytic interfaces [5,6]. One alternative, which has yielded promising results, has been the infiltration-based approach, which involves the introduction of the Ni phase into a porous YSZ scaffold via a liquid precursor through capillary action, followed by calcination [7, 8].

For example, Buyukaksoy et al obtained a polarization resistance of ca. 0.1 $\Omega.cm^2$ per electrode at 800 °C, under 3% H_2O – 97% H_2 gas mixture flow [8]. However, this method requires numerous infiltration/calcination steps, (e.g., 60 cycles in the case of 5), which necessitates significant optimization for implementation into mass production [8].

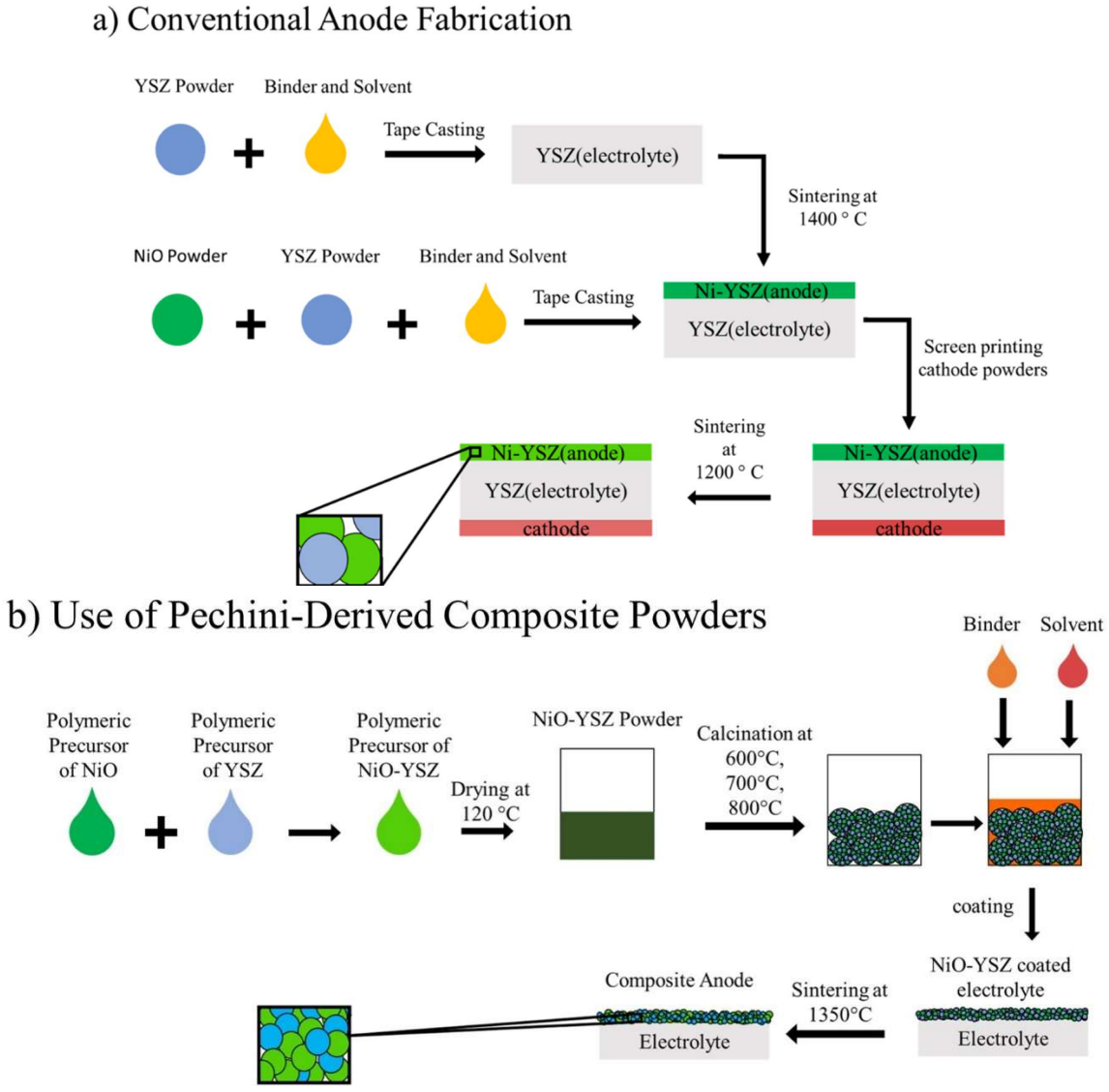

Figure 1. Schematic representation of Ni-YSZ anode fabrication via a) the conventional route involving the sintering of powder mixtures and b) the route involving the sintering of composite powders derived by a Pechini method.

Another approach to obtain Ni-YSZ anodes with long TPBs has been the synthesis of composite powders consisting of intimately mixed, nanoscale NiO and YSZ crystals for sintering [9]. For this purpose, Han et al calcined a mixture of commercial YSZ powder and a Ni-precursor solution [10], while Mohebbi et al tried the microwave-assisted combustion method [11]. Keech et al adopted a sol-gel based approach [12], which involved the mixing of Ni and YSZ precursor solutions. Grgicek et al [13] and Li et al [14] synthesized NiO-YSZ powders via co-precipitation, while Ringuede et al used combustion synthesis [15]. Razpotnik et al used the ethylene glycol-based Pechini technique and successfully synthesized NiO-YSZ powders [16]. Interestingly, among the above-mentioned literature, only two studies have investigated the electrochemical activity of the composite powder-derived anodes [12-15], one of which reported a ca. fifty-fold lower electrochemical performance than those fabricated by infiltration [12].

In the present work, we report on the synthesis of NiO-YSZ composite powders via an ethylene glycol-based Pechini method, due to its simplicity and thereby, scalability (Figure 1b). Long TPB lengths in the as-sintered anode, due to the molecular level mixing of the constituent cations allowed by this fabrication method is expected. In addition, for the first time in the literature, we correlate the calcination temperature used to obtain the NiO-YSZ powders from Pechni precursor, first to the microstructure, then to the electrochemical performance of the sintered Ni-YSZ anode.

2. EXPERIMENTAL

2.1. Powder synthesis and symmetrical half-cell fabrication

Polymeric precursors of NiO and YSZ were prepared separately. To obtain a polymeric NiO precursor $Ni(NO_3).6H_2O$ (Sigma-Aldrich, crystals or chunks) was first dissolved in distilled water. Then, ethylene glychol (Alfa Aesar, 99%) was added to the solution to achieve a 0.04:1 cation to ethylene glycol molar ratio. The resultant clear solution was stirred at 80°C until added water evaporated and polymerization took place. The YSZ polymeric precursor was prepared in a similar way. $Y(NO_3)_3.6H_2O$ (Alfa Aesar, 99.9%) and $ZrOCl_2.8H_2O$(Sigma-Aldrich, ≥99.5%) were dissolved in distilled water to achieve an Y:Zr molar ratio of 0.16:0.84. Then, etyhlene glycol was added to the solution maintaining a cation to ethylene glycol molar ratio of 0.02 to 1 and the resultant solution was stirred on a hot plate at 80°C until the water evaporated. To obtain a polymeric NiO+YSZ polymeric precursor, the NiO and YSZ solution precursors were mixed in appropriate amounts that would yield NiO-YSZ powders with a 60:40 volummetric ratio. To obtain crystalline powders, the NiO/YSZ gels dried from the NiO+YSZ precursor solutions were calcined at 600, 700 and 800°C for 4 hours, in air.

The electrolyte substrate was fabricated by die-pressing 0,7 grams of commercial YSZ powder (TOSOH TZ-8Y) at 0,15 ton/m² pressure, using a die with a 1 cm diameter. For better compaction, the die-pressed pellets were subjected to cold isostatic pressure (CIP) at 200 MPa. The obtained pellets were sintered at 1400°C for 2 hours, in stagnant air.

To form the symmetrical half-cells, synthesized NiO-YSZ composite powders were mixed with α-Terpineol (Alfa-Aesar, ≥96%) and 2-Butoxyethanol (Sigma-Aldrich) to obtain inks. These inks were deposited onto the electrolyte surfaces and sintered at 1350°C for 2 hours, in air, to ensure bonding among the powders and at the powder/electrolyte interface.

2.2. Sample characterization

Particle size distributions of the synthesized powders were measured by laser diffraction method (Malvern Mastersizer 2000). Phase analyses of NiO, YSZ and NiO-YSZ powders were performed by x-ray diffraction (XRD, Rigaku D-Max 2200) using Cu Kα radiation source. Morphological and microstructural analysis of powders calcinated 600-800 for 4 hours carried out with scanning electron microscopy (SEM, Philips XL 30 SFEG).

Electrochemical impedance spectroscopy (EIS) measurements were performed at 500-750°C, in stagnant air at the 5×10^{-2} - 10^{5} Hz frequency range, using ±10 mV excitation voltage (Gamry

Potentiostat, Reference 3000). NiO paste consisting of a mixture of Ni (II) oxide powder (Alfa-Aesar, 99%), α-Terpineol (Alfa-Aesar, ≥96%) and 2-Butoxyethanol (Sigma-Aldrich) was applied onto the anodes. Electrical contacs were made by attaching Nickel wires (Alfa-Aesar, 0.25 mm diameter, 99.98%) onto the electrodes using Ceramabond adhesive.

3. RESULTS AND DISCUSSION

3.1. Powder characteristic

To determine the phase evolution of NiO-YSZ composite powders, first, the crystal structure of gels dried from separate polymeric NiO and YSZ precursors after calcination at 600, 700 and 800°C for 4 hours was determined by x-ray diffraction (XRD). Peaks belonging to cubic NiO (PDF: 03-065-5745) as well as metallic Ni phase (also cubic in structure, PDF:00-004-0850) were observed, calcination upon even at 600°C (Figure 2a). With increasing calcination temperature metallic Ni transformed into cubic NiO (Figure 2a). Cubic YSZ phase (PDF: 00-030-1468) was obtained at all calcination temperatures (Figure 2b). The peak widths decreased with increasing calcination temperature, indicative of increasing crystal size (Figure 2b). The XRD patterns obtained from a mixture of polymeric NiO and YSZ precursors, showed that cubic NiO and YSZ phases crystallized separately and no solid solution formation took place, regardless of the calcination temperature (Figure 2c). The YSZ peaks typically had wider peaks in comparison to those that belonged to NiO (Figure 2b).

To determine the effect of mixing the polymeric NiO and YSZ precursors on the crystallization behavior of the respective phases, the average crystallite sizes of NiO and YSZ phases were calculated from XRD patterns using the Scherrer equation (1),

$$D_p = \frac{0.9\lambda}{B\cos\theta} \quad (1)$$

where λ is x-ray wavelength, θ is the diffraction angle and B is the full width at half maximum intensity and Dp is the average crystallite size.

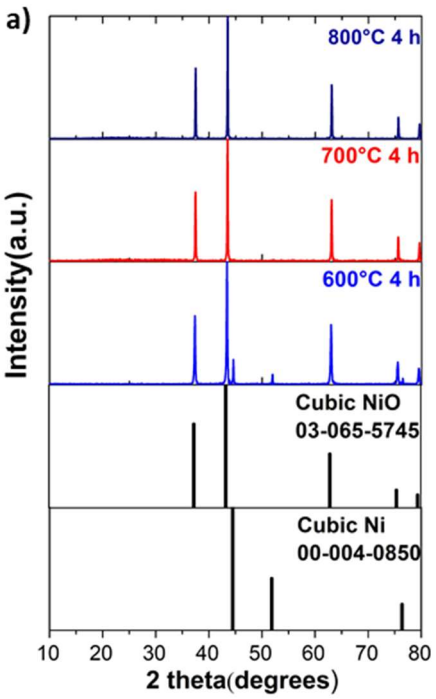

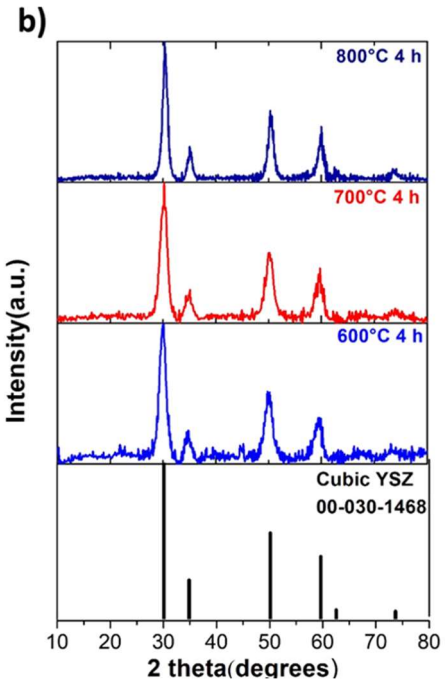

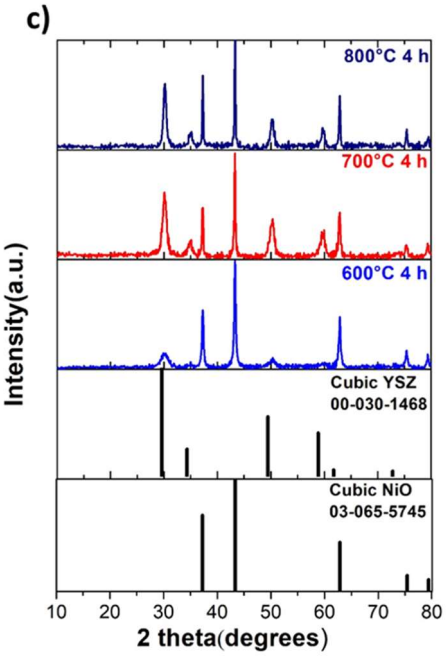

Figure 2. X-ray diffraction patterns obtained from gels dried from a) NiO, b) YSZ and c) NiO-YSZ polymeric precursors, calcined at 600, 700 and 800 °C.

Figure 3 shows the changes in the crystallite sizes of NiO and YSZ phases with increasing calcination temperature, in the cases of separate and mixed polymeric precursors. The crystallite size of NiO and YSZ phases increased with increasing calcination temperatures in both separate and mixed precursor solution cases (Figure 3). The crystallite size of the NiO phase was significantly smaller in the mixed precursor solution case in comparison to single precursor derived NiO (Figure 3). Evidently, the presence of Zr^{4+} and Y^{3+} ions in the solution hindered the clustering of Ni^{2+}, thereby resulting in smaller NiO crystals in comparison to those obtained from a separate NiO precursor. The inhibition of long-range order NiO crystal formation by the addition of Zr^{4+} and Y^{3+} ions to the solution suggests the formation of a nanocomposite powder. On the other hand, no significant effect of polymeric NiO precursor addition on the YSZ phase evolution was determined within the measurement accuracy of our equipment (Figure 3). Overall, NiO-YSZ composite powders with average NiO and YSZ crystal sizes in the ranges of 26-37 and 7 - 11 nm, respectively, were obtained using a mixture of polymeric NiO and YSZ precursors upon calcination at 600-800 °C.

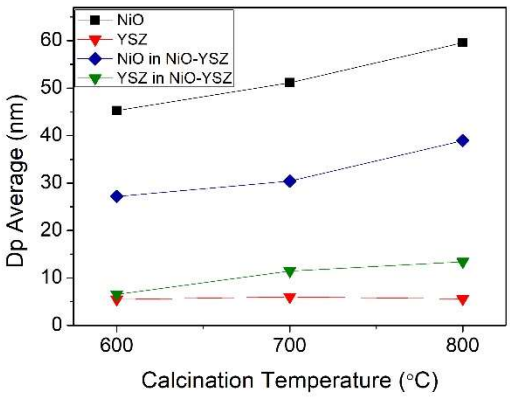

Figure 3. Average crystallite size of NiO and YSZ phases in NiO, YSZ and NiO-YSZ powders as a function of calcination temperature.

NiO-YSZ powders synthesized by microwave-assisted combustion were reported to have average crystal sizes ranging from 8 to 33 nm and from 14 to 32 nm for NiO and YSZ respectively, depending on the pH from of the solution [11]. On the other hand, Razpotnik et al. reported that average crystal sizes of NiO and YSZ varied between 42 to 48 nm and 6 to 15 nm, respectively, when a Pechini method, similar to the one adopted in the present study, was used [16]. However, the NiO and YSZ crystal sizes reported here for the Pechini-derived composite powders are somewhat smaller than those reported in Refs 11 and 16, suggesting a more intimate mixing and thus, potentially longer triple phase boundaries.
Another important characteristic of the synthesized powders that may be detrimental to the electrochemical activity is the particle size distribution. Laser diffraction measurements revealed that the amount of submicron-sized particles decreased with increasing calcination temperature (Figure 4a). The average particle size of NiO-YSZ powders was 897 ±31, 1073 ±16 and 1313 ±19 nm at 600, 700 and 800 °C, respectively (Figure 4b), which is significantly smaller than the particle size values reported for the Pechini-derived NiO-YSZ powders reported in the literature (average particle size 8.6-14.9 µm in REF-16). Particle sizes somewhat smaller than those reported in the present work have been achieved by Han et al (0.4 – 0.7 µm), who mixed a NiO precursor solution with fine, commercial YSZ powder [10] to achieve NiO-YSZ composite powders. Overall, the relatively small crystallite

and particle sizes were obtained in this present study via Pechini process. Thus, favourable microstructure upon sintering and thus, promising electrochemical activity can be expected.

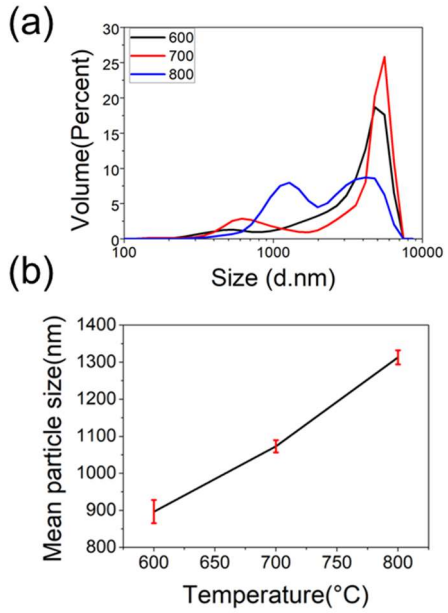

Figure 4. Effect of calcination temperature on a) particle size distribution and b) average particle size of NiO-YSZ powders.

3.2. Microstructural Analysis

Symmetrical half-cells were fabricated by depositing inks containing NiO-YSZ powders calcined at 600, 700 or 800 °C, followed by sintering at 1350 °C. The obtained NiO-YSZ composites were then reduced under 10% H_2-90%Ar flow, at 750 °C before microstructural analysis by scanning electron microscopy (SEM), to simulate electrochemical analysis conditions. Cross-sectional SEM images collected from the fracture surfaces of Ni-YSZ anode layers fabricated from NiO-YSZ powders calcined at 600-800 °C are provided in Figure 5. Ni-YSZ anode fabricated from powders calcined at 600 °C appears to be homogeneous in general, with only two larges (a few microns in size) particle chunks visible (shown with arrows in Figure 5a). With increasing powder calcination temperature, both the number and size of these large particle chunks increase significantly (Figures 5b and c), in agreement with the particle size analysis in Figure 4. Although the distribution of Ni and YSZ phases within these particle chunks may be homogeneous and provide long triple phase boundaries (as seen in Figures 5d-f), they are hardly sinterable, thus, their extent of bonding to the electrolyte and to their surrounding particles are quite poor (Figures 5b and c). The deteriorated contact between the powders and the electrolyte substrate is also evident when the low-magnification top surface images of anodes using powders calcined at 600 and 700 °C (Figures 5g and h) to those using powders calcined at 800 °C (Figure 5i). Consequently, electrochemical activity is expected to decrease with increasing powder calcination temperature.

3.3. Electrochemical Activity

The assessment of the electrochemical activities of Ni-YSZ anodes prepared from Pechini-derived NiO-YSZ powders was performed by electrochemical impedance spectroscopy (EIS) analyses of symmetrical half-cells at 500-750 °C, under humidified 10%H_2 – 90%Ar flow. Figures 6a-c depict the Nyquist curves obtained at 750 °C from Ni-YSZ anodes fabricated from composite powders calcined at 600-800 °C, with corresponding Bode diagrams provided in the insets. At this operating temperature, the EIS responses consisted of two distinct semi-circles, indicating two separate electrochemical processes (Figures 6a-c). Therefore, an equivalent circuit consisting of one resistor (Rs) connected in series to two other resistors (R1 and R2), both of which is also connected in parallel to two constant phase elements (Q1 and Q2) was used to fit the EIS data (Figures 6a-c). Here, Rs describes the resistance to ionic conduction through the YSZ electrolyte, while R1/Q1 and R2/Q2 describes the high and low frequency processes, respectively. At lower operating temperatures, only one semi-circle was observed (data not shown), therefore fitting procedures were performed using an equivalent circuit consisting of only one R/Q element connected in series to Rs.

Table 1 provides the resistance and frequency values obtained from the equivalent fitting of the EIS data, in addition to the capacitance values calculated from these two parameters. Rs values, evidently, increased from 4.5 to 5.1 $\Omega.cm^2$ with increasing powder calcination temperature (Table 1).

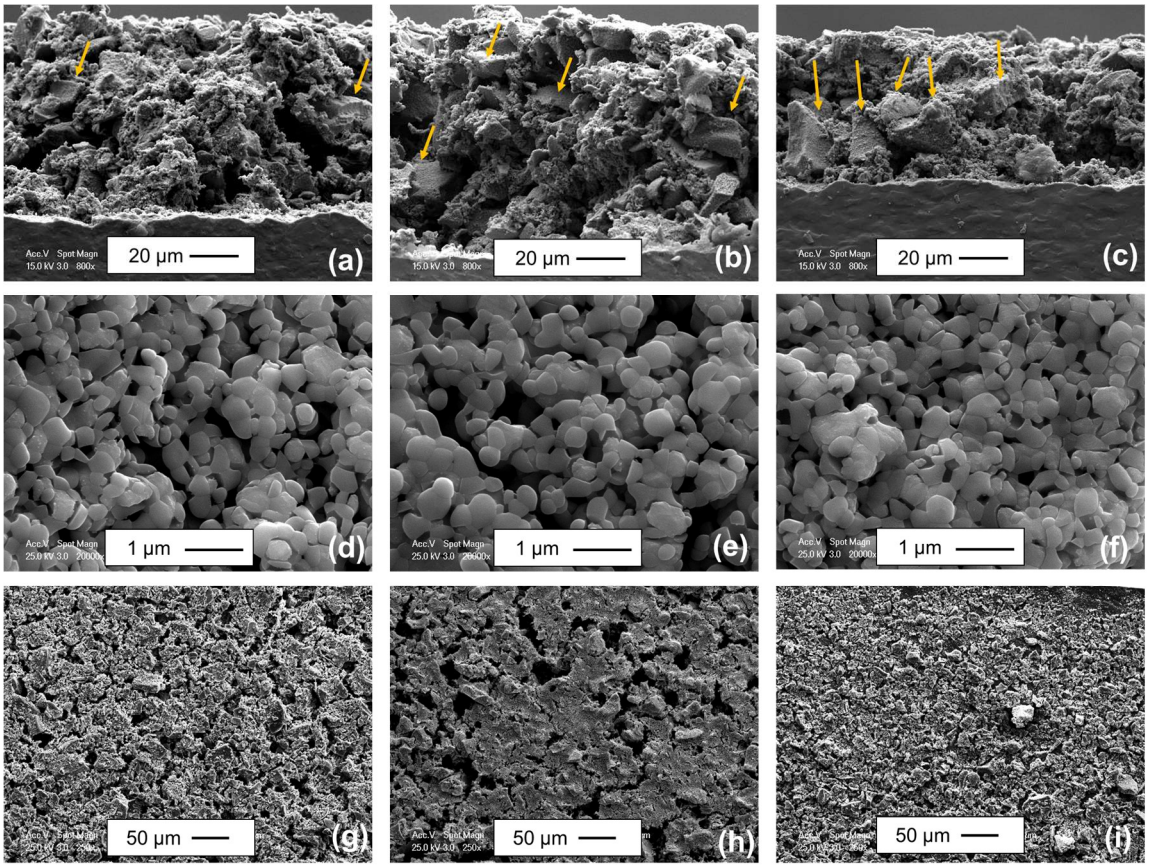

Figure 5. Scanning electron microscopy images collected from Ni-YSZ anodes fabricated from powders calcined at a, d, g) 600, b, e, g) 700 and c, f, i) 800 °C. The images in the first row are collected from the fractured cross-sections, while those in the second and third rows are collected from the top surfaces of the anodes.

Considering that i) the conductivity of YSZ electrolyte substrates are the same and ii) the thickness variation in the electrolyte substrates is below ca. 5%, the increase in ohmic resistance is considered to have originated from the poorer physical, hence electrical contact in Ni-YSZ anodes fabricated from larger particles. In a similar way, the sizes of both high and low frequency semi-circles also increased with increasing powder calcination temperature. R1 increased from 1.83 to 4.78 $\Omega.cm^2$ when the powder calcination temperature was increased from 600 to 800 °C. The capacitance values associated with the high frequency process were in the 10^{-6} F/cm^2 range, which have been ascribed to the double layer capacitance at the Ni/YSZ interface [17,18]. The low capacitance associated with the high-frequency arc suggests that the charge transfer at the triple phase boundary dominated the total polarization resistance. The low frequency process, on the other hand had capacitance values in the10^{-3} F/cm^2 range, which was ascribed to the hydrogen adsorption/desorption processes at the Ni surface [17]. The fact that R1 is significantly larger than R2 in all cases indicates that charge transfer at the triple phase boundary is the process limiting the hydrogen oxidation rate in all samples.

Rtotal values were determined by adding R1 and R2, which was then divided by two, to obtain the total polarization of one electrode (Ranode) in the symmetrical two-electrode cell (Table I). The lowest Ranode value obtained was 1.16 $\Omega.cm^2$, in the case of Ni-YSZ anode prepared from NiO-YSZ composite powders calcined at 600 °C. This value corresponds to a better electrode performance than reported in REF-17, in which Dasari et al obtained an Ranode value of 1.63 $\Omega.cm^2$ at 750 °C from Ni-YSZ anode fabricated by co-sintering a mixture of NiO and YSZ

powders. On the other hand, infiltration of Ni into porous YSZ scaffolds resulted in lower Ranode values than those reported here, i.e., 1.3 and 0.1 Ω.cm^2 at 700 and 800 °C, respectively [8,19]. Despite the higher electrochemical activity of the infiltrated Ni-YSZ anodes, the necessity for numerous infiltration/drying cycles for their fabrication (as many as 60 cycles in the case of REF-8) renders them unsuited for scaling up.

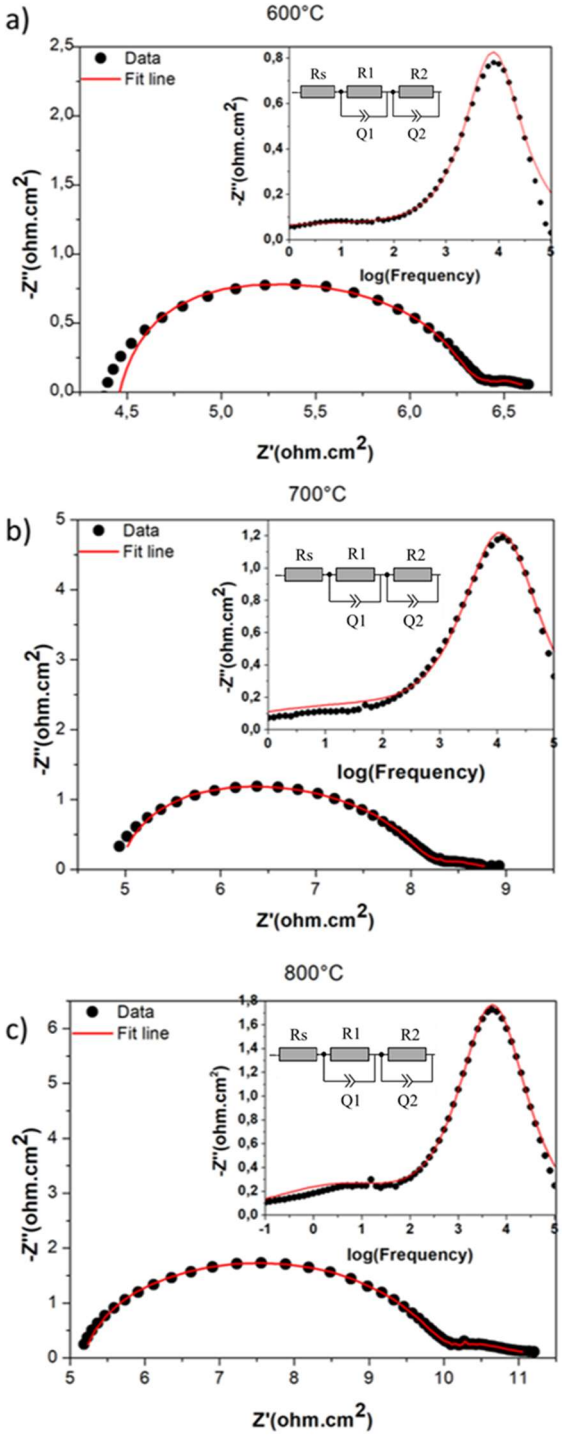

Figure 6. Electrochemical impedance spectroscopy data obtained from anodes fabricated using powders calcined at a) 600, b) 700 and c) 800°C in the form of Nyquist and Bode (insets) diagrams. Note that the filled circles and the red lines show the data points and the fit curves, respectively.

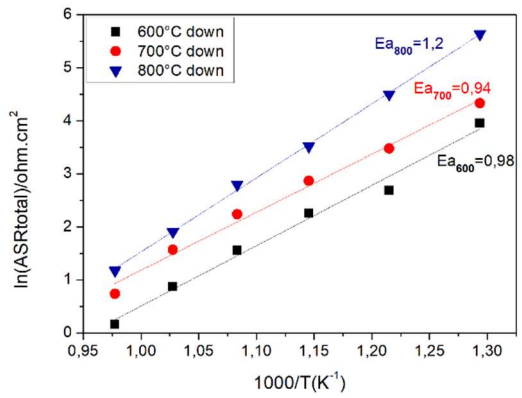

Figure 7. Temperature dependence of Ranode, measured in the cooling regime.

Figure 7 shows a comparison of the temperature dependencies of the Ni-YSZ anodes fabricated from composite NiO-YSZ powders synthesized by the Pechini method. Activation energies of anodes fabricated from NiO-YSZ composites calcined at 600, 700 and 800°C were determined as 0.98, 0.94 and 1.20 eV, respectively. The activation energies of the charge-transfer dominated polarization resistances of Ni-YSZ anodes have been reported to lie in the 1.00-1.30 eV range [8, 19], due to the combined effects of oxygen ion transport through the YSZ network (which has an activation energy of 0.9-1.1 eV [19]) and electron transfer at the triple phase boundary (which has activation energy of ca. 1.30 eV [19, 20]). The activation energies of Ranode obtained from anodes with NiO-YSZ powders calcined at 600 and 700 °C are close to that of oxygen ion transport through the YSZ network, while the activation energy of Ranode obtained from anodes with NiO-YSZ powders calcined at 800 °C is close to that of the electron transfer at the triple phase boundary. The effect of powder calcination temperature on the Ranode activation energy is likely related to the quality of the powder/electrolyte substrate contact. Specifically, coarse powders obtained by calcination at 800 °C resulted in a poor powder/electrolyte substrate

contact, resulting in the dominance of the resistance of the high activation energy-electron-transfer process.

4. SUMMARY

Symmetrical half-cell anodes were fabricated from NiO-YSZ composite powders, successfully synthesized via an ethylene glycol-based Pechini method. This method provided molecular level mixing of cations and hence, resulted in long triple phase boundaries. X-ray diffraction (XRD) analyses revealed that calcination of the gels dried from the polymeric NiO-YSZ precursors at 600 °C resulted in cubic Ni, NiO and YSZ phases, while the metallic Ni was absent when the powders were calcined at 700 or 800 °C. XRD measurements also revealed that mixing of the NiO and YSZ precursors yielded a NiO phase with smaller crystallites in comparison to the unmixed NiO precursor, upon calcination.
Sintering of anode layers deposited onto dense YSZ electrolytes at 1350 °C resulted in a homogeneous, mostly agglomerate-free microstructures when powders calcined at 600 °C were used. On the other hand, large agglomerates were detected in anodes fabricated from NiO-YSZ powders calcined at 700 and, especially 800 °C. Anode polarization resistances of 1.17, 2.09 and 3.10 Ω.cm² at 750 °C were achieved upon the electrochemical impedance spectroscopy measurements of anodes containing powders calcined at 600, 700 and 800 °C, respectively, which reflected the effect of powder calcination conditions on the performance of the sintered anode.

Acknowledgements

This work has partially been supported by The Scientific and Technological Research Council of Turkey (Project No: 217M031).

Research and Publication Ethics

The authors state that, in this work, they have complied with international research and publication ethics.

Ethics Committee Approval

This paper does not require any ethics committee permission or special permission.

Conflict of Interests

Authors declared no conflict of interest.

Table 1. Summary of resistance, frequency and capacitance values extracted from the equivalent circuit fitting of impedance data collected at 750 °C.

Powder calcination temperature (°C)	Rs (Ω.cm²)	$f_1$summit (Hz)	R_1 (Ω.cm²)	C_1 (F/ cm²)	$f_2$summit (Hz)	R_2 (Ω.cm²)	C_2 (F/ cm²)	Rtotal (Ω.cm²)	Ranode (Ω.cm²)
600	4.50	17100	1.83	5.09×10^{-6}	153	0.50	2.08×10^{-3}	2.33	1.16
700	4.76	26800	3.10	1.92×10^{-6}	180	1.08	8.19×10^{-3}	4.18	2.09
800	5.06	15300	4.78	2.18×10^{-6}	25	1.42	4.56×10^{-3}	6.20	3.10

REFERENCES

[1] A.H. Karim, K.-Y. Park, T.H. Lee, S.A. Muhammed Ali, S. Hossain, H.Q.H.H. Absah, J.-Y. Park, A.K. Azad, "Synthesis, structure and electrochemical performance of double perovskite oxide $Sr_2Fe_{1-x}Ti_xNbO_{6-\delta}$ as SOFC electrode," Journal of Alloys and Compounds, vol. 724, pp. 666-673, 2017.

[2] S.C. Singhal, K. Kendall, "High temperature solid oxide fuel cells: fundamentals, design, and applications" Elsevier Science Ltd, ISBN 1-85617-387-9, Oxford, UK, 2003.

[3] S.Tao, J. T. S. Irvine, "A redox-stable efficient anode for solid-oxide fuel cells," Nature Materials, 2(5), 320–323, 2003.

[4] A. Sarikaya, V. Petrovsky, F. Dogan, "Effect of the anode microstructure on the enhanced performance of solid oxide fuel cells," International Journal Hydrogen Energy, vol. 37, pp. 11370-11377, 2012.

[5] B. S. Prakash, S. S. Kumar, S.T. Aruna, "Properties and Development of Ni/YSZ as an anode material in solid oxide fuel cell: A review", Renewable and Sustainable Energy Reviews 36, 149-179, 2014.

[6] J. Mizusaki, H. Tagawa, T. Saito, T. Yamamura, "Kinetic studies of the reaction at the nickel pattern electrode on YSZ in H_2–H_2O atmospheres," Solid State Ionics, vol. 70/71, pp. 52–58, 1994.

[7] T. Klemenso, K. Thyden, M. Chen, H.-J. Wang, "Stability of Ni-yttria stabilized zirconia anodes based on Ni-impregnation," Journal of Power Sources, vol. 195, no 21, pp. 7295-7301, 2010.

[8] A. Buyukaksoy, S.P. Kammampata, V. I. Birss, "Effect of porous YSZ scaffold microstructure on the long-term performance of infiltrated Ni-YSZ anodes," Journal of Power Sources, vol. 287, pp 349-358, 2015.

[9] P. Tiwari, S. Basu, "Ni infiltrated YSZ anode stabilization by inducing strong metal support interaction between nickel and titania in solid oxide fuel cell under accelerated testing," International Journal of Hydrogen Energy, vol. 38, no. 22, 9494-9499, 2013.

[10] K.R. Han, Y. Jeong, H. Lee, C.-S. Kim, "Fabrication of NiO/YSZ anode material for SOFC via mixed NiO precursors," Materials Letters, vol. 61, pp. 1242-1245, 2007.

[11] H. Mohebbi, T. Ebadzadeh, F.A. Hesari, "Synthesis of nano-crystalline (Ni/NiO)–YSZ by microwave-assisted combustion synthesis method: The influence of pH of precursor solution, Journal of Power Sources, vol. 178, pp. 64-68, 2008.

[12] P.G. Keech, D.E. Trifan, V.I. Birss, "Synthesis and Performance of Sol-Gel Prepared Ni-YSZ Cermet SOFC Anodes," Journal of The Electrochemical Society, vol. 152, no. 3, pp. A645-A651, 2005.

[13] C.M. Grgicak, R.G. Green, W.-F. Du, J.B. Giorgi, "Synthesis and Characterization of NiO–YSZ Anode Materials: Precipitation, Calcination, and the Effects on Sintering," Journal of American Ceramic Society, vol. 88, no. 11, pp. 3081-3087, 2005.

[14] S. Li, R. Guo, J. Li, Y. Chen, W. Liu, "Synthesis of NiO-ZrO_2 powders for solid oxide fuel cells," Ceramics International, vol. 29, pp. 883-886, 2003.

[15] A. Ringuede, D. Bronine, J.R. Frade, "Assessment of Ni/YSZ anodes prepared by combustion synthesis," Solid State Ionics, vol. 146, pp. 219-224, 2002.

[16] T. Razpotnik, J. Macek, "Synthesis of nickel oxide/zirconia powders via a modified Pechini method," Journal of

European Ceramic Society, vol. 27, pp. 1405-1410, 2007.

[17] H.P. Dasari, S.-Y. Park, J. Kim, J.-H. Lee, B.-K. Kim, H.-J. Je, H.-W. Lee, K. J. Yoon, "Electrochemical characterization of Ni-yttria stabilized zirconia electrode for hydrogen production in solid oxide electrolysis cells," Journal of Power Sources, vol. 240, pp. 721-728, 2013.

[18] S. Dierickx, J. Joos, A. Weber, E. Ivers-Tiffée, "Advanced impedance modelling of Ni/8YSZ cermet anodes," Electrochimica Acta, vol. 265, pp. 736-750, 2018.

[19] A. Buyukaksoy, V.I. Birss, "Comparison of the Electrochemistry of Ni Thin Film and Ni-YSZ Composite Anodes Fabricated by Polymeric Precursor Deposition," Journal of The Electrochemical Society, vol. 163, no. 13, pp. F1350-F1357, 2016.

[20] V. Sonn, A. Leonide, and E. Ivers-Tiffée, "Combined deconvolution and CNLS fitting approach applied on the impedance response of technical Ni8YSZ cermet electrodes," Journal of the Electrochemical Society, vol.155, no. 7, pp. B675-B679, 2008.